Phase-Locking the Photoinjector Laser to the ERLP Accelerator RF

G J Hirst[1] and L B Jones[2]

Report against EUROFEL DS3 Deliverable D3.16

This work has been partially supported by the EU Commision in the Sixth Framework Program, Contract No. 011935 – EUROFEL, and by STFC ASTeC

[1]STFC Central Laser Facility, Rutherford Appleton Laboratory, Chilton, Didcot OX11 0QX, UK

[2]STFC Accelerator Science and Technology Centre, Daresbury Laboratory, Keckwick Lane, Daresbury, Warrington WA4 4AD, UK

Phase-Locking the Photoinjector Laser to the ERLP Accelerator RF

G J Hirst and L B Jones

1. INTRODUCTION AND SYSTEM DESCRIPTION

The Energy Recovery Linac Prototype (ERLP) [1] is a pulsed electron accelerator sited at the UK's STFC Daresbury Laboratory. The machine layout is shown in fig 1. Electron bunches are generated in a DC gun, compressed using an RF-buncher and accelerated in two 1.3GHz superconducting (SC) modules, designated Booster and Linac. After acceleration the electrons are transported round a race-track shaped path and returned to the Linac module where energy is recovered from them before they are dumped. The transport path includes a bunch compressor (chicane) to increase the peak current followed by a wiggler in which cavity FEL action will take place. The machine has been built to allow accelerator development, particularly in support of the 4GLS proposal, and plans are also in place to exploit it as a photon and electron source in its own right.

For the ERLP to operate effectively the electron bunches from the gun must be launched into the RF-powered elements (the buncher and the SC modules) with well-controlled timing relative to the RF phase. The electron source in the gun is a Cs:GaAs photocathode illuminated by optical pulses from a green (532nm) drive laser system. The electron bunch timing depends directly on the timing of the laser pulses. The degree to which the laser pulse timing is controlled, i.e. its synchronisation with respect to the accelerator RF, is the subject of this report.

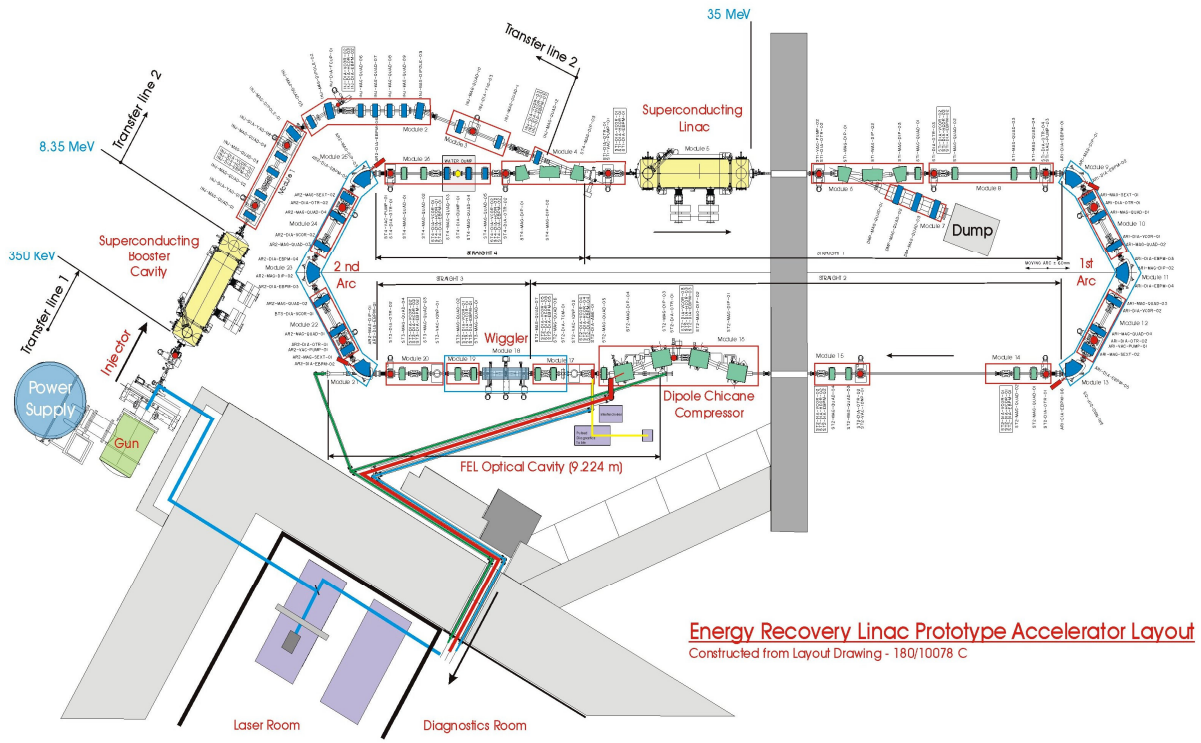


Figure 1: Layout of the ERLP accelerator.

1.1 The Accelerator RF

The high-power RF for the accelerator is supplied by inductive output tubes (E2V model no IOT116LS and CPI Inc model no CHK51320W) which are driven by a solid-state amplifier chain. The primary RF source which feeds this chain is a low-noise crystal oscillator (Wenzel Inc VHF PLO model no 500-15309) coupled to a series of multipliers and dividers. A schematic and a photograph of this front end system are shown in fig 2. In addition to its 1.3GHz output a secondary output at 81.25MHz is provided as a reference source for the photocathode drive laser.

The maximum phase noise from the Wenzel oscillator is specified as -125dBc/Hz at 100Hz offset, -155dBc/Hz at 1kHz offset and -170dBc/Hz at 10kHz offset. In principle the processes of multiplication and division will increase (or decrease) these noise levels by 20logN, where N is the factor by which the frequency changes. In practice each module will contribute some additional noise, but the exceptional performance of the oscillator should not be degraded significantly.

Since the aim of the synchronisation scheme is to lock the timing of the electron bunches at the photocathode to the phase of the RF *in the accelerating cavities* it might be thought that a direct monitor of the cavity RF, rather than an output derived from the low-level front end, would be the best reference source for the laser. This would have the advantage that phase variations arising in any part of the RF amplification and transport chain would be tracked by the control loop. Such phase

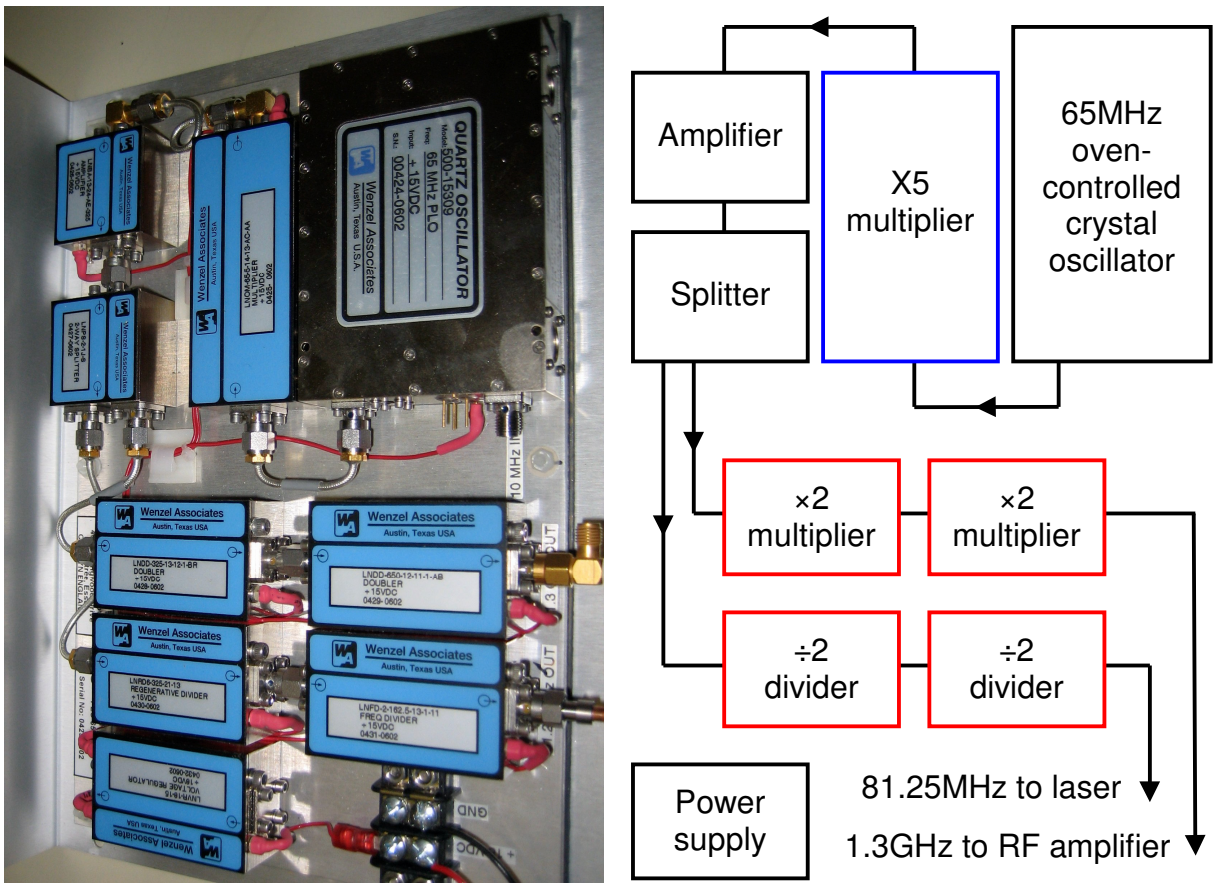


Figure 2: Photograph and schematic of the ERLP RF front end.

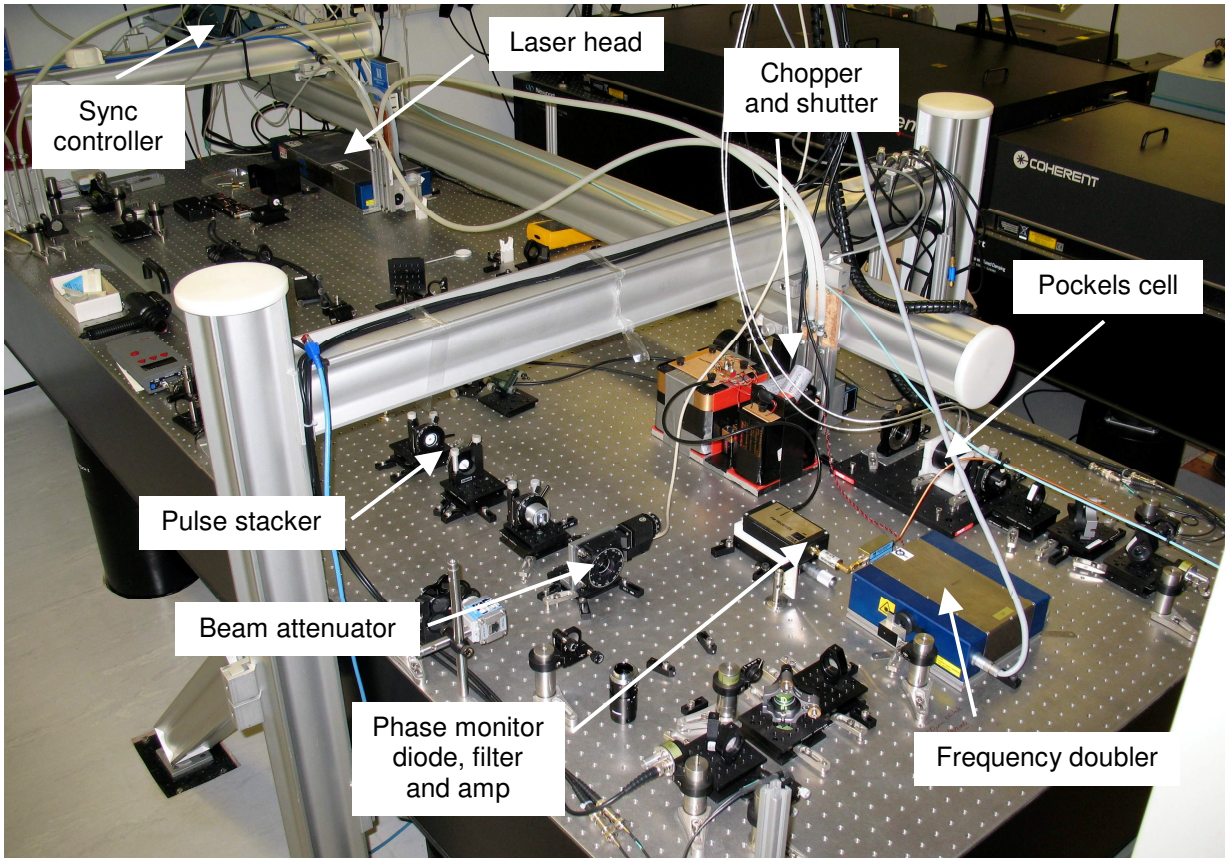
variations are known to exist. They can be caused, for example, by the dependence of the IOT phase shift on the HT voltage [2]. A cavity monitoring scheme might well be implemented on a machine such as 4GLS but in the case of ERLP there are practical considerations which, to date, have prevented this. One is that in a development environment there will necessarily be periods when the electron gun needs to be tested independently of the whole suite of RF-powered elements. Another important point is that for thermal and RF power reasons the only element which has so far carried electron current (the RF-buncher) has had to be operated in pulsed mode. Deriving a signal from the buncher cavity field would result in a pulsed reference which would not be suitable for laser synchronisation. All of the results presented in this report have therefore been taken with the laser locked either to the 81.25MHz output from the RF front end or to an equivalent stand-alone reference source.

Included in the RF system is a transport cable which carries the reference signal to the laser. For ease of access when the accelerator is operational the laser is housed in a room outside the radiation shield wall. To avoid long transport paths for the high power RF the bulk of the RF system, including the front end, is located close to the SC modules i.e. inside the shield wall. This requires the physical length of the transport cable to be more than 35m. The air temperature inside the laser room is controlled but this is not the case for the environment through which the transport cable passes. Diurnal temperature changes of several degrees might be anticipated, especially if large access doors need to be opened, and seasonal changes could be 2-3 times this. To avoid timing drifts arising from temperature dependence of the cable delay it was decided to use phase-stabilised cable for this application. The selected cable has silver-plated copper conductors and an expanded PTFE dielectric (ATM Inc, type CF-135). With a transit time of ~4ns/m the overall cable delay is ~140ns. The manufacturer's specification for the temperature coefficient of delay is –400ppm over the temperature range -65ºC to 120ºC i.e. ~2.2ppm/ºC. So the use of phase-stabilised cable should limit the timing variation to ~300fs/ºC or ~1ps diurnally.

1.2 The Laser System

A schematic and a photograph of the laser system (High Q Laser Production GmbH, model IC-532-5000) are shown in fig 3. The laser head produces a CW train of 7-8ps FWHM pulses at a rate of 81.25MHz and an average power of >10W. The wavelength is 1064nm. Limitations on available RF power and on ionising radiation dose mean that the ERLP cannot be operated CW so a time-structuring assembly (chopper, shutter and Pockels cell) is used to slice macropulses from the CW train. The macropulse length can be varied from one pulse to 8125 pulses (100μs) and the macropulse rate can be adjusted from 1Hz to 20Hz. After time-structuring the laser beam passes through a frequency doubler which converts up to 50% of the pulse energy to the green (532nm). A variable attenuator is then used to control the beam power. Following this an optional polarisation pulse stacker can lengthen the pulse from 5-6ps up to 25-30ps. Following the stacker the beam travels to the photocathode via an image-relaying transport system which can be adjusted to vary the beam size.

The optical transport path is piped, both for safety reasons and to minimise the effects of air movements. The transverse position of the laser beam on the cathode can be adjusted using stepper motor-driven translation stages under two of the turning mirrors. Fig 3 also shows the elements used to synchronise the laser to the accelerator RF and to monitor its synchronisation.



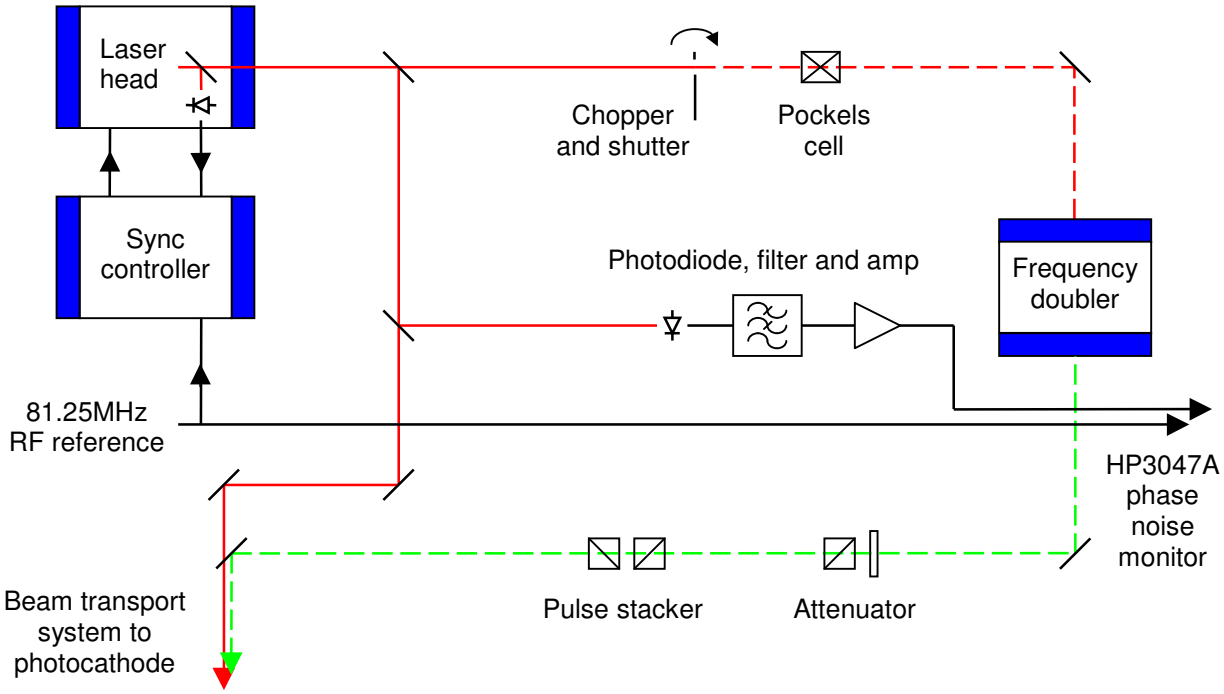


Figure 3: Layout of the photoinjector laser system, including phase noise monitor.

The laser head is a single box which contains diode-pumped Nd:YVO_4 oscillator and amplifier modules. The oscillator is passively modelocked using a semiconductor saturable-absorber mirror. The laser head baseplate is water-cooled with the coolant temperature maintained within ±0.1ºC. The inside of the laser head is shown in fig 4.

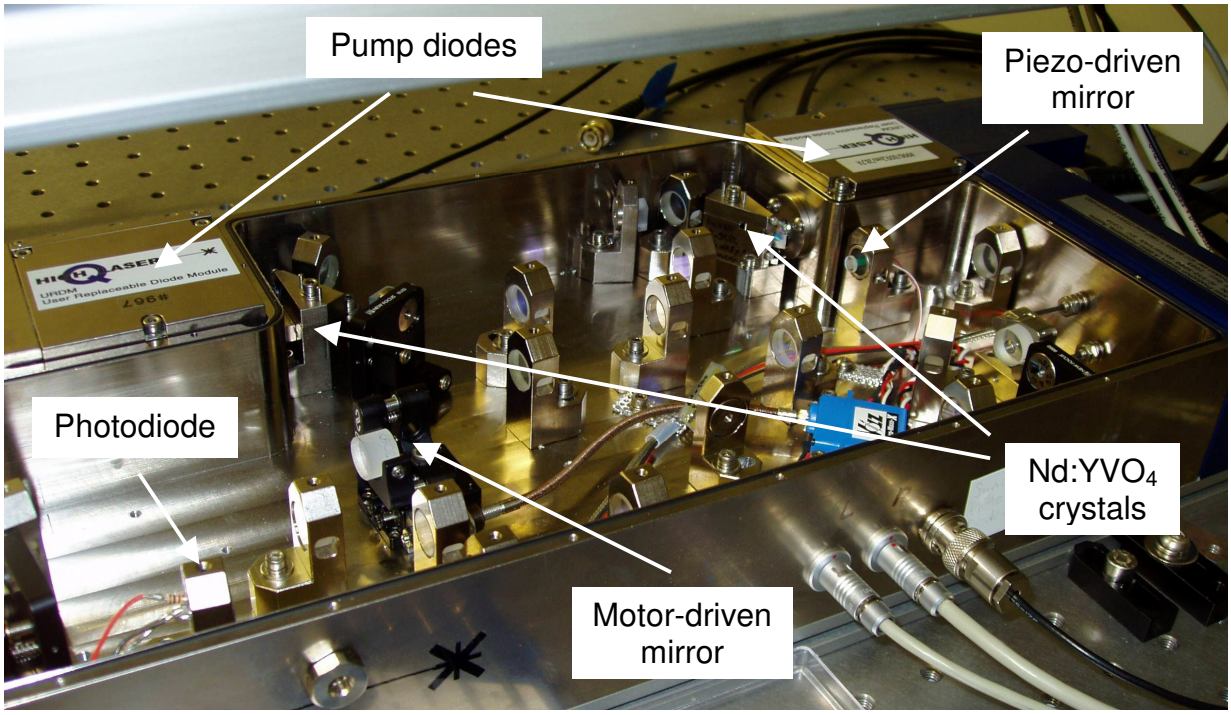


Figure 4: Inside view of the laser head showing the moving mirrors and the timing monitor photodiode.

The laser oscillator can be synchronised to an external RF reference using the associated “sync controller”. The first element in this is a phase detector which extracts the phase error between the RF reference and the signal from a monitor photodiode inside the laser head. The error signal is fed into a phase-locked loop (PLL) feedback control system. This adjusts the laser oscillator frequency (and hence the phase) by changing the length of the laser cavity. Large changes are made by a motor-driven mirror which can alter the frequency by ~10kHz (0.012%). The position of this mirror is set during the lock acquisition process and is only altered thereafter if a second, piezo-driven mirror reaches the end of its control range. Once the control loop is closed, this piezo-driven mirror is used to maintain it dynamically. The upper limit of the loop bandwidth is a few hundred hertz, which is comfortably below the electromechanical resonant frequency of the piezo element.

It is generally the case that PLL feedback control will suppress a system’s intrinsic noise by a factor determined by the PLL filter characteristics. Requirements for stability and other considerations set upper limits to this factor, so the lowest levels of output noise can only be achieved by minimising the intrinsic noise levels present before the control system is switched on. Potential sources of such noise include EM pickup e.g. in the detector and PLL electronics, acoustics and vibrations which can affect the length of the laser cavity and beam transport paths, and transient variations in the laser medium properties.

To minimise the EM pickup the laser room has been constructed, as far as possible, as a Faraday cage. The wall and ceiling panels are skinned with galvanised steel and the joints between them are covered with electrically conductive tape. The floor contains a layer of copper foil which is connected along its edges to the walls. Power, signal and communications cables which penetrate the Faraday cage are filtered as

far as possible. Within the laser room attention has been paid to minimising local EM noise by using high quality cables on Pockels cell drivers and separating the cables to the sync controller from those carrying high or rapidly-changing currents.

Acoustic noise in the laser room comes primarily from the rotating chopper and the 1-20Hz shutter which make up the laser time-structuring assembly. In principle this could be reduced by enclosing these items with a sound absorbing material (e.g. commercial foam/lead sheet composite such as McMaster-Carr Supply Company part no 53995T34). Noise from fans in electrical equipment is relatively low because most of this equipment is housed either outside the room or in overhead racks with sliding doors, primarily to reduce the heat load on the air conditioning plant. As well as reducing the noise at source, the acoustic sensitivity of the laser was also damped by attaching self-adhesive high-density noise barrier sheet (T.Mat Engineering Ltd part no P02/D05) to the laser head top-plate.

As well as airborne noise the laser is also sensitive to mechanical vibration. It is therefore mounted on a honeycomb optical table with tuned mechanical dampers (Newport corporation model no M-RS2000-410-12) which is itself mounted on rigid isolators (Newport corporation model no PL-2000-423.5, with the pneumatic elements uninflated). For maximum beam stability the isolators pass through the laser room's false floor and are seated straight onto the building's concrete floor slab. In this part of the building the floor slab rests directly on the bedrock which is a 300m thick layer of Bunter sandstone. The relative stability of this material was one of the reasons that Daresbury was chosen as the site of an accelerator laboratory in the 1960's.

The optical table top is an effective vibration damper but vibration levels would still have been raised if mechanically noisy components had been mounted on the table itself. An independent gantry has therefore been constructed from aluminium rails (Newport corporation X95 system) and the chopper and shutters are suspended from this. The gantry is supported from the laser room floor and walls but does not touch the table top. The limited apertures of the chopper blade slot and some of the shutters could have led to alignment problems, given the different thermal expansion coefficients of the aluminium gantry and the steel table isolators. However close control of the laser room air temperature prevents this from becoming an issue.

2. SYNCHRONISATION REQUIREMENTS

The level of synchronisation required for the ERLP photoinjector laser depends on the machine's operating mode. Most of the time it will be used to study a wide range of accelerator performance characteristics (electron beam brightness, energy recovery efficiency, cryogenic accelerator operations etc). For most of this work the photoinjector laser synchronisation needs only to be good enough to support basic machine operation.

The required timing jitter can be estimated using a very simple model of electron transport through the accelerator. The electron bunch (modelled as 1024 particles with uncorrelated Gaussian distributions in energy and time) is assumed to leave the gun and buncher with a mean energy of 350keV, a 1% rms energy spread and a length of 4ps rms. The Booster has a harmonic accelerating field with 8MV amplitude and adjustable phase. The transfer line between the Booster and the Linac introduces a

small amount of dispersion with an R_{56} of 0.03m. The Linac amplitude and phase are set at 27MV and -9° respectively and the bunch compressor has an R_{56} of 0.28m. The return arc decompresses the bunch with an R_{56} of -0.28m before return to the Linac for energy recovery.

Time was not available to simulate all of the ERLP's operating scenarios. Instead two of the more sensitive ones were chosen to investigate the effects of laser jitter – FEL operation and Compton scattering. The ERLP FEL is sensitive to timing jitter for two reasons. The most obvious is that the photon pulse in the FEL cavity will only be amplified if it overlaps with consecutive electron bunches. This requires the jitter to be less than the electron bunch duration (in fact significantly less, since FEL gain occurs only near the electron current peak). However it must be remembered that this aspect of FEL operation will only be affected by relatively rapid timing changes. The photon lifetime in the cavity is short, varying from ~0.4μs to ~1.2μs depending on the type of mirrors used. On timescales longer than this the photon timing will simply track any changes in the electron timing. In addition the maximum ERLP macropulse length is just 100μs so timing variations slower than this will also have no effect. These results suggest that contributions to the laser jitter at frequencies below ~100kHz can be disregarded. Since this is where much of the laser phase noise is (see below) it seems likely that the direct effect of timing jitter will be insignificant. More important will be an indirect effect – the influence of laser timing on the peak electron current.

Results from the transport model are given in figs 5 and 6. These show the electron current and the energy/arrival time relationship after the bunch compressor for different timings of the photoinjector laser. Three things are clear. Firstly when the laser timing is optimised the electron bunch is compressed to ~700-800fs rms. Secondly the electron current peak moves by a relatively small amount in time as the laser pulse timing shifts (the reason for this is obvious from fig 6 which shows that for electrons on the near "vertical" section of the curve, changes in the initial timing tend to affect energy rather than arrival time). Finally the laser timing has a major effect on the peak amplitude of the current.

Since the current peak moves by much less than its width, the effect of this on FEL operation can be neglected. However the effect of the amplitude changes is significant. One of the purposes of the FEL is to "disrupt" the electrons' properties so that transport and energy recovery of electron bunches occupying a large volume of phase space can be studied. If it is to influence a useful fraction of the electrons then the FEL needs to be well above threshold for much of the current pulse. A plausible criterion might be that the integrated area under that part of the trace where the current is above 40A (a level which gives reasonable FEL gain) should contain at least 50% of the bunch charge. Analysis of current traces corresponding to different drive laser timings shows that this criterion is satisfied provided the laser timing is within ±3ps of the optimal value. For this to be the case for more than 95% of the laser pulses requires the laser timing jitter to be less than 1.5ps rms.

The COBALD experiment [3] will generate X-rays by Compton scattering of the optical pulses from a multi-TW laser off the ERLP electrons. The interaction point will be after the bunch compressor since this is where the shortest X-ray pulses can be produced. The X-ray yield depends strongly on the spatio-temporal overlap between the laser photons and the electrons and also on the fluence in each of the beams. There are

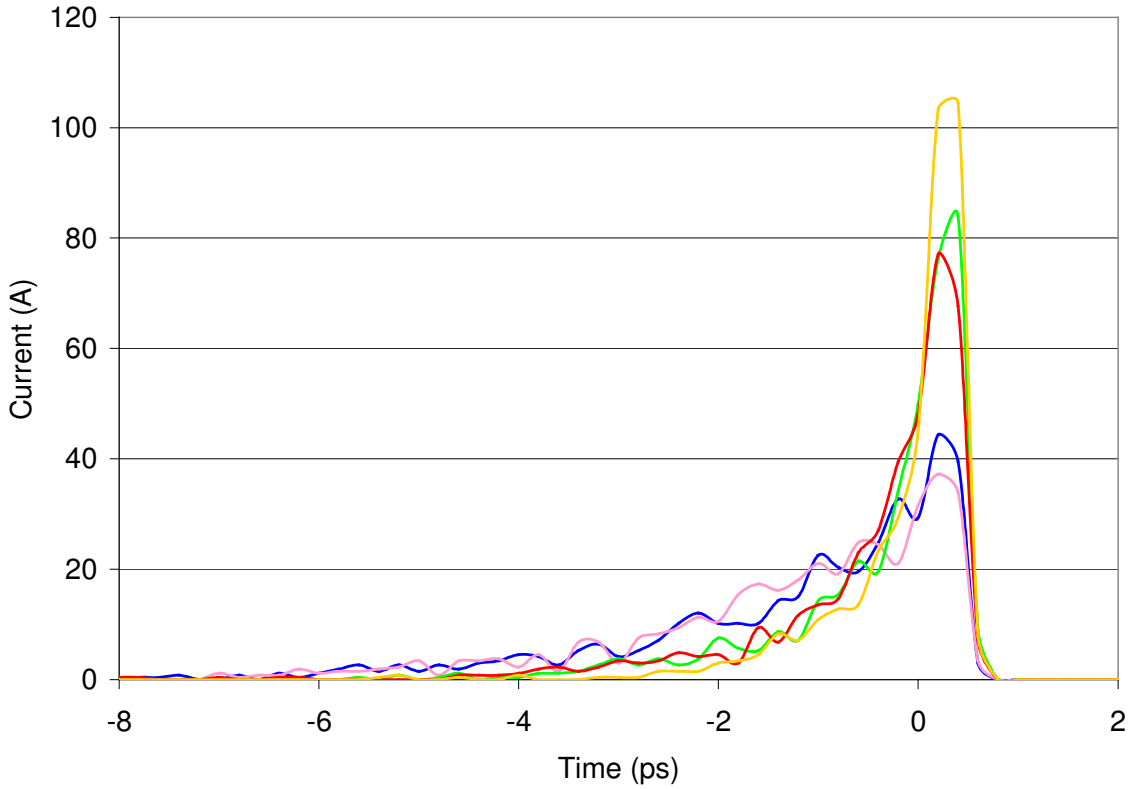


Figure 5: Electron current after the bunch compressor for different drive laser timings --6ps (pink), -3ps (red), 0ps (yellow), +3ps (green) and +6ps (blue).

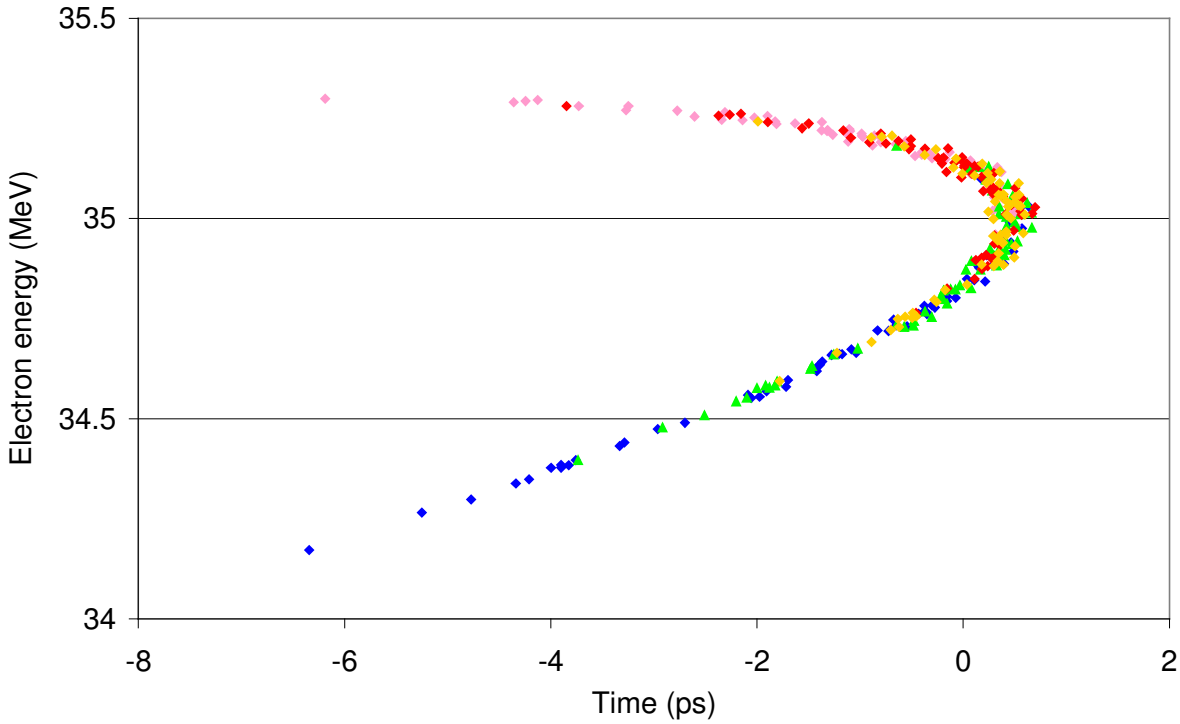


Figure 6: Relationship between energy and arrival time for electrons launched with five different drive laser timings (64 electrons from each bunch are shown with colours corresponding to the laser timings in fig 5).

two possible scattering geometries – head-on and transverse (90°). In the head-on geometry the multi-TW laser will be focused with a Rayleigh range, z_R, of ~1.5mm. The laser beam divergence angle will be several times greater than that of the electron beam so changes in the laser intensity will be the major consequence of any timing shift between the photons and electrons. In reality the jitter of the multi-TW laser itself may be significant in this respect, but this will not be considered here. As was shown in fig 5, the main effect of photoinjector drive laser jitter is to stretch the electron bunch in time rather than to move it. So instead of all of the electrons colliding with the photons close to the common focus of the two beams, some of the electrons will interact at points further away. Assuming a Gaussian beam, the laser fluence on axis will be proportional to $1/(1+(z/z_R)^2)$ where z is the axial position of the interaction point. Clearly the fluence will fall as |z| increases but the electron beam (whose divergence is relatively small) will overlap more and more with just the high intensity central part of the laser beam. This slows the fall-off in the X-ray yield which can be shown, by radial integration, to be proportional to $1/(2+(z/z_R)^2)$. On this basis electrons which interact at $z=z_R$ will still generate X-rays with 67% of the efficiency achieved at z=0. It is clear from fig 5 that even with a photoinjector laser timing shift of 6ps practically all of the electrons will arrive at the IP within 5ps of the nominally correct time. This corresponds to a physical displacement of 1.5mm i.e. z_R. So in the head-on geometry the overall reduction in X-ray yield for even a large change in photoinjector laser timing will be small.

In the transverse geometry the laser pulses and the electron bunches will be timed to overlap at the peak of the electron current. The effect of photoinjector laser timing jitter will be to reduce the size of this peak, with a corresponding fall in the X-ray yield. The choice of an acceptable fall-off of the X-ray output will always be arbitrary, but if it is required that for 95% of the shots the peak electron current is more than 50% of the "zero timing offset" value, then the photoinjector laser jitter will need to be less than 2.5ps rms.

The timing jitter requirements of 1.5ps rms for effective FEL operation and 2.5ps rms for adequate Compton X-ray yield should be comfortably met by commercial laser oscillators. However in addition to these basic operational needs the ERLP will also be used to study synchronisation issues themselves. Here the aim will be to examine the processes which lead to timing jitter in a real accelerator environment and to eliminate them, where possible, and control them, where not. Clearly there is no "target figure" for timing jitter in this part of the programme. The aim will simply be to understand its sources and to reduce them as far as possible.

3. DIAGNOSTICS

The laser system itself is supplied with two synchronisation diagnostics. The first is a simple LED indicator on the sync controller which reflects the status of the phase-locked loop electronics. It flashes during the process of lock acquisition and then illuminates continuously once the loop is locked.

The second diagnostic is the sync controller's "Phase" signal which is derived from the output of the phase detector. It gives a direct measure of the phase difference between the reference RF and the photodiode monitor inside the laser. The signal can be displayed on an oscilloscope to give real-time information about the phase shift

between the reference RF and the laser pulse train. Equally it can be fed into a spectrum analyser to give frequency domain information about the phase noise.

The Phase signal can be calibrated by observing it when the PLL is not locked. Under these circumstances the laser pulses oscillate into and out of phase with the RF reference. The Phase signal also oscillates at the beat frequency and its sensitivity near the zero crossing, which is where it operates when the PLL is locked, is related to its unlocked amplitude V_{pp} and to the RF period τ_{RF} by the equation:

$$\text{Phase sensitivity} = \pi \times V_{pp} / \tau_{RF} \qquad (1)$$

V_{pp} is typically 20V and τ_{RF} is 12.3ns so the Phase monitor sensitivity is 5.1mV/ps.

The third, and most sophisticated, synchronisation diagnostic is a commercial phase noise monitoring system (Hewlett-Packard model no HP3047A). A thorough and very helpful description of this and of its use for measuring laser synchronisation is given in [4]. More detailed information about the system itself is available in the many hundreds of pages of HP technical documentation which go with it. In view of this only a relatively brief description will be given here.

A schematic of the phase noise measurement system is shown in fig 6. An obvious, but important point to note is that the HP3047A measures *relative* phase noise between its two inputs. This is in contrast to the utilities available on some spectrum analysers which measure, nominally, the absolute noise of a source (in fact they measure the noise relative to their internal master oscillators, which are assumed to be perfect). The ability to perform relative measurements is a critical requirement for synchronisation testing when the performance of the systems under test becomes comparable with the best commercial oscillators.

The first element in the system is the photodiode/filter/amplifier assembly which converts the optical output from the laser into a near-sinusoidal RF signal at 81.25MHz. The photodiode circuit is identical to the one used by the authors of [4]. Batteries are used to bias the diode and to power the amplifier with minimum noise. The diode's cathode is connected to ground by a 560Ω resistor and is coupled to the 50Ω filter via a 0.1μF capacitor. It is also connected to ground through an 18kΩ resistor and a 0.47μF capacitor in series, with the voltage across the capacitor being used to monitor the average current. Two photodiodes were tested for linearity and the effects of power loading. Linearity was checked by irradiating each diode with a fraction of the beam from the laser, attenuated using calibrated ND filters. (These are typically only specified at optical wavelengths and their performance can be very different at 1.06μm.). The photodiode output was amplified as it would be for normal operation and the resulting signal level was measured into a 50Ω load. The results are shown in fig 7.

The first test was carried out using the external low-noise RF amplifier (Wenzel Inc, LNAF-120-0-15-AC-L) but without the separate low-pass filter (Mini-Circuits, SLP-100). The amplifier itself has an internal low-pass output filter with a 120MHz cut-off frequency. So although it is fed with an 81.25MHz train of 2-3ns pulses from the photodiode its output consists only of the fundamental component of this plus the

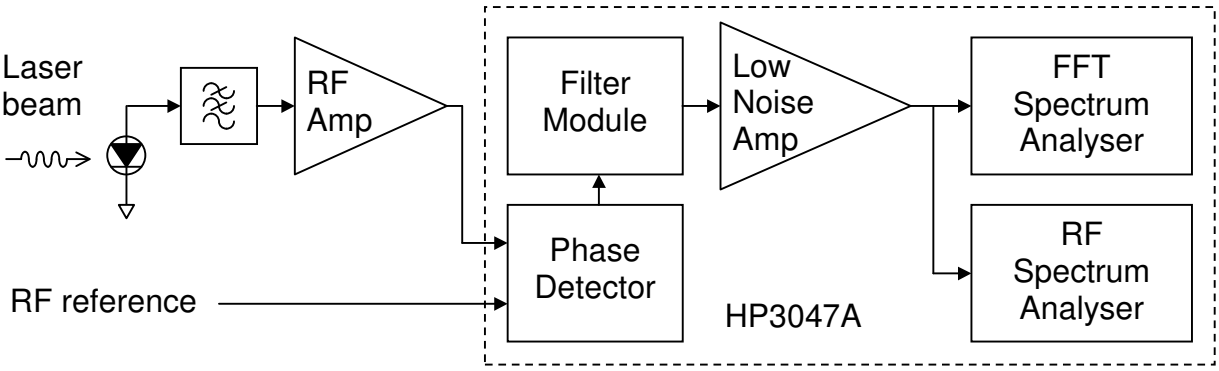


Figure 6: Schematic of the phase noise measurement system.

sidebands which carry the noise information (see below). It is clear from fig 7 that while the responses without the filter are linear for signals below ~300mV (3dBm) they quickly saturate at levels above this. What is happening is that the amplifier is saturating on the peaks of the short pulses. When the Mini-Circuits filter is added the situation improves greatly. It has a 98MHz cut-off frequency so it reduces the signal to an 81.25MHz sinusoid plus the noise sidebands *before* the amplifier, whose full range can then be used to amplify the fundamental component. As a consequence the saturation limit rises. With the filter in place the output is linear up to at least 2.1V rms (19.5dBm).

The two photodiodes give similar output levels. The G8376 unit is made of InGaAs which has approximately ten times the photosensitivity of the silicon S3883 at 1.06µm.

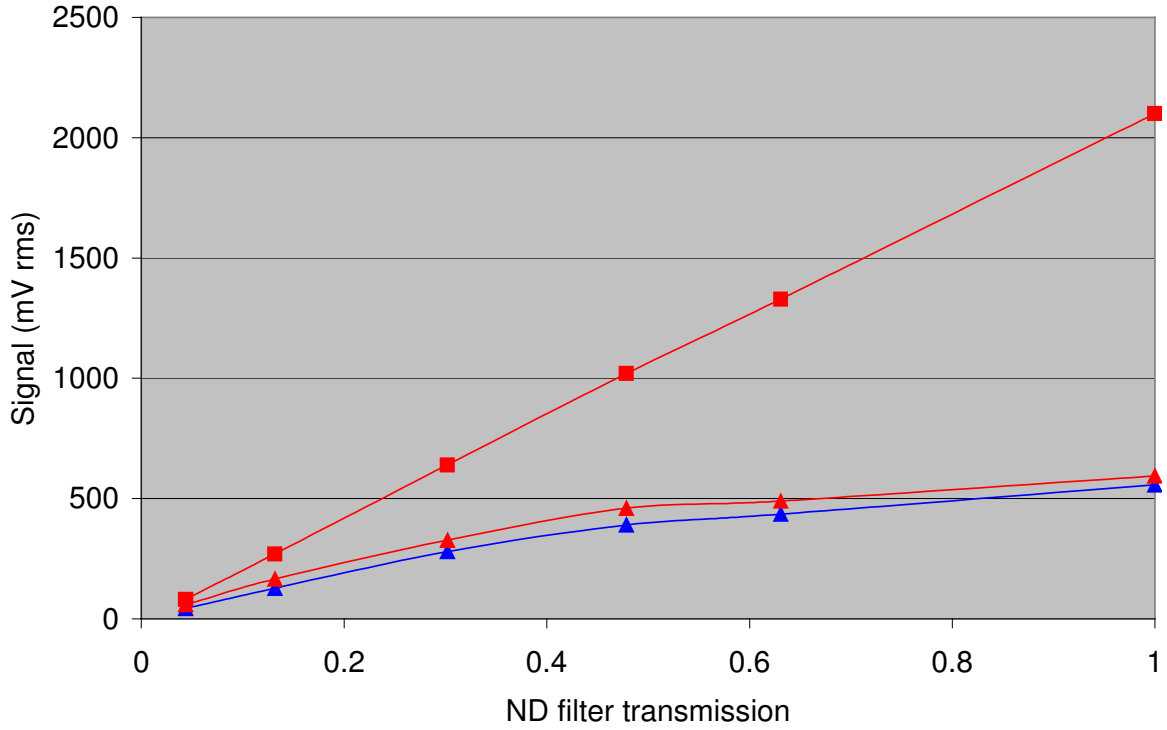


Figure 7: Response of the phase monitor photodiode/filter/amplifier assembly to a 1.06µm laser pulse train at 81.25MHz, with filter (squares) and without (triangles) using Hamamatsu S3883 (blue) and G8376-05 (red) photodiodes.

However, for a given active area, InGaAs diodes are inherently slower than silicon ones. So to achieve a frequency response of ~100MHz the InGaAs diode needs to be smaller. The active area of the G8376 is nearly an order of magnitude less than that of the S3883, which almost cancels out the material's photosensitivity advantage. All of the measurements reported here were carried out using the G8376-05 diode, with -18V DC bias, and the SLP-100 filter.

The hardware elements of the HP3047A are a phase detector, a signal conditioning suite (filters and amplifiers) and two spectrum analysers. These are interconnected using semi-rigid coaxial cable (RG402) to minimise noise pickup. A fourth (and vital) element, not shown in fig 6, is the computerised control and data acquisition system which sets the hardware up, monitors and optimises the operating parameters as the data is being acquired and processes the results, taking into account calibration, measured noise levels etc. The principle on which the phase error is detected is the generation of a baseband (difference frequency) output from a low-noise passive mixer (M/A Com Inc, type M9H) fed by the two input signals which are arranged to be in quadrature with one another. If the signals are simply mixed with an arbitrary phase relationship between them then the baseband output spectrum will contain contributions arising from both phase and amplitude noise on the inputs. The amplitude term can be eliminated either by operating in strict quadrature, the approach adopted in the HP3047A, or by feeding the mixer with high harmonics of the 81.25MHz signals. In the latter case the ratio of the phase contribution to the amplitude one increases in proportion to the harmonic number and the phase noise eventually becomes dominant. The details of the quadrature approach are discussed in [4]. Its effectiveness for this application is assessed in Section 4 below.

By definition it is not possible to maintain exact quadrature (i.e. an exact 90° relative phase) between two waveforms which are subject to relative phase noise. The HP3047A measures the phase error in real time and generates a proportionate output voltage. If required this can be used to control the frequency of the reference oscillator so that quadrature is maintained. The detector then senses phase noise only. Of course the measured noise is reduced by this process, but the HP3047A software accounts for this and corrects the results. Fortunately the noise between the RF reference and the ERLP photoinjector laser is sufficiently low that this technique is not needed. All the measurements reported here were carried out simply by establishing quadrature manually and then leaving the system undisturbed while the measurement process ran. Quadrature was set by physically adjusting the length difference between the two input signal paths. The reference path was made up entirely of fixed lengths of cable. The last part of the laser beam path could be adjusted by moving the photodiode, which was mounted on a translation stage, towards or away from the laser. The HP3047A would accept length differences of the order of a few hundred microns from the exact quadrature point, corresponding to time differences of the order of 1ps.

The output of the phase detector is low-pass filtered to eliminate all but the baseband component. The amplitude of this is determined by the input signal levels which are limited at the high end of the range by the mixer. If signal levels are low then the HP3047A's low-noise amplifier can be used to increase them, but the finite mixer noise floor means that low input signal levels always degrade the signal-to-noise ratio. This is why external low-noise amplifiers are also used in the input paths.

After the filtering and amplification the phase noise signal is measured using the systems' two spectrum analysers. Measurements are taken over fixed frequency ranges, starting at the high frequency end, and then stitched together to produce the full spectrum. Multiple measurements may be taken and averaged. The length of time required for the full acquisition depends on the number of averages and on the chosen lower frequency limit, since effective sampling of low-frequency noise is inherently time-consuming. Acquisition times of 15-20 minutes are not unusual. If the phase noise changes on the timescale of the acquisition then sudden steps can appear in the final spectrum. These occur at the points where two scans over neighbouring frequency ranges meet. This happens at frequencies either of 1×10^{n}Hz or 4×10^{n}Hz and sharp features at these points may simply reflect changes occurring between acquisitions.

The spectrum analysers work simply as tuned narrowband power meters. They measure power per unit bandwidth which, for the purposes of phase noise analysis, is usually expressed with respect to the overall power in the carrier. The name of this quantity is "noise spectral density" and its units are dBc/Hz. Phase noise is mostly broadband and uncorrelated, so it is usually legitimate for the analyser to derive the noise spectral density by dividing the measured power at a given frequency setting by the corresponding filter bandwidth. However the real phase noise spectrum will often also include narrowband features, known as spurs. The way that the HP3047A treats these merits some discussion.

The spectrum analyser produces measurements at adjacent frequencies, the spacing between them being several times less than the filter bandwidth. If the actual bandwidth of a spur is much narrower than the analyser's filter bandwidth then it will contribute to the measured power for a number of adjacent frequency points. However at each point the analyser will divide the measured power by the filter bandwidth. The consequence of this is that if the analyser treats the spur signal in the same way that it treats all the other signals, then the integrated area under the noise spectral density graph, which has the dimensions of relative power (dBc), will be correct. This is important because the rms timing jitter, which is what characterises synchronisation, is derived from the integrated spectral density via the formula:

$$\Delta t_{rms} = (2/\omega_0).(\int L(f)\ df)^{1/2} \qquad (2)$$

where ω_0 is the carrier frequency and $L(f)$ is the noise spectral density. The correct evaluation of the integral is critical in calculating the timing jitter.

Unfortunately the output from the HP3047A is open to misinterpretation. The data processing package includes routines which attempt to identify spurs in the measured spectrum (in practice these routines are reasonably effective, but not completely so). When the spectrum is presented graphically the broadband element is shown as a solid line, but for features identified as spurs the line is shown dashed. Because spurs are, by definition, narrower than the resolution bandwidth (the filter bandwidth) the system chooses *not* to divide the measured power by the bandwidth for them. The dashed curve is therefore a measure of power, not of noise spectral density (despite the abscissa label on the graph !). This has the advantage that the total power in the spur can be read directly off the graph, since it corresponds to the peak of the dashed curve. But the disadvantage is that if the area under the dashed curve is integrated then it will *not* give a correct value for $\int L(f)\ df$. Fig 8 shows, all on the same vertical

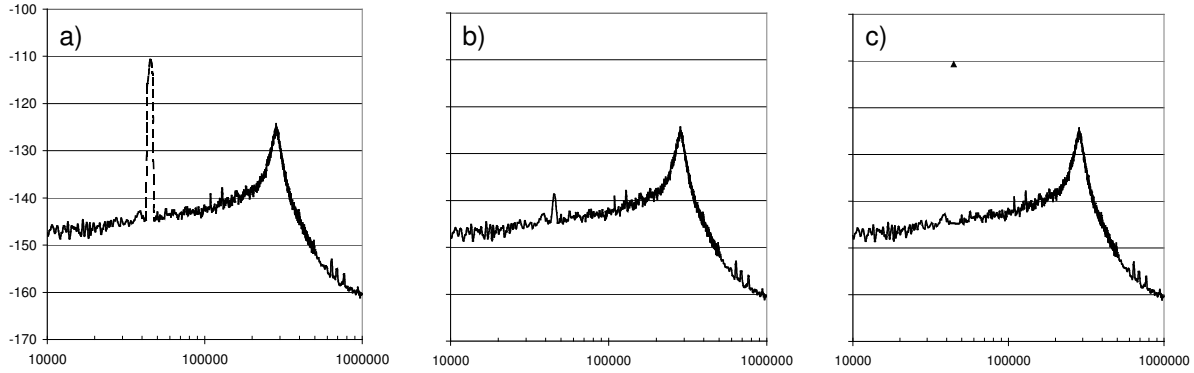


Figure 8: Graphical representations of phase noise spectral density (dBc/Hz) including a 45kHz spur a) as shown by the HP3047A system, b) as "measured" without treating the spur data differently and c) with the spur separated from the broadband data.

scale, a) the way the HP3047A actually presents a section of real data from one of the ERLP measurements, b) the way it treats the same data (as measured power divided by bandwidth) before identifying the spur and c) an alternative way of presenting the data which separates the unresolved narrowband spur from the broadband noise and marks it as an isolated data point. The correct integral of the noise spectral density can be obtained either by integrating b) directly or by integrating c) and adding the spur power (-110.7dBc) afterwards. Obtaining it from a) is not so straightforward.

The HP3047A system needs to be comprehensively calibrated before measurements can begin. Reference sources internal to the system can be used for some of the calibrations. But accounting for the sensitivity of the phase detector requires an external signal. Such a signal can be derived in a number of ways, but the one used here is the so-called "beat note" technique which is very similar to the approach used to calibrate the laser sync controller's Phase output. The system is set up exactly as it would be for a phase noise measurement but the sync controller is then switched off. This causes the laser pulse rate to shift slightly with respect to the reference RF. The phase detector output then oscillates at the beat frequency and the HP3047A hardware can measure the amplitude of this oscillation and calculate the system's sensitivity (phase slope). The value for the above setup was typically ~0.4V/rad.

4. RESULTS

4.1 Diagnostics

Considering the simplest of the diagnostics first – the LED on the High Q sync controller– this has been found to be a useful indicator of the PLL status, but not a completely reliable one. Operational experience has shown that the sync controller's PLL can lose lock for a number of reasons. In most cases the LED then goes out. However there is at least one PLL failure mode (see below) where the LED does not go out, despite the loss of lock. This "failure to danger" means that the LED signal cannot be used as an input source for any machine protection system.

The second of the High Q diagnostics – the Phase output signal from the sync controller – seems to be a reliable indicator of the true phase error. Because it works

in the time domain it is also good at revealing transient effects. However there are two significant practical issues with its use. The first is that the signal level is small. The sensitivity of 5.1mV/ps means that the typical laser timing jitter, which might be a few hundred femtoseconds rms, generates a Phase signal of just a few millivolts. This can be comparable with background laboratory noise levels e.g. at the 50Hz line frequency, especially if the signal is monitored on a 1MΩ oscilloscope input (the Phase output will not drive 50Ω). So although Phase gives a reasonable indication of performance it is difficult to use it as a tool to detect small changes.

The second issue relates not to the Phase signal itself but to the way it is monitored. Timing jitter is typically expressed as the rms phase error. If the signal is displayed on a digital oscilloscope then the rms level can be calculated and displayed in real time using the oscilloscope's internal signal analysis software. However care is needed to ensure that this shows the full picture. The phase noise spectrum is very broad, covering at least 6 orders of magnitude in the frequency domain. It is important to be sure that the digital sampling process and the algorithms used to calculate the rms signal level can accommodate this very wide range.

The important performance parameters characterising the third diagnostic - the phase noise measurement system - are a) its ability to maintain quadrature while a measurement is being taken and b) its noise floor. As described above, the system components which influence quadrature are those which control the lengths of the two input paths – the electrical one which carries the RF reference signal to the phase detector and the optical and electrical one which carries the laser beam to the photodiode and the photodiode output to the phase detector. The final arrangement, using phase-stabilised cable for the RF reference and semi-rigid coaxial cable for the filtered and amplified photodiode signal has proved to be very robust. Once the photodiode is positioned to the quadrature point it stays stable for hours. If quadrature is lost this was usually because of a failure of the laser synchronisation.

The noise floor of the phase noise measurement system sets the lower limit to the timing jitter which can be measured. Several of the system components contribute to the overall noise floor level. These include the photodiode, which is subject to shot noise, the RF amplifiers and the spectrum analysers, which suffer from instrumental noise, and the interconnections, which can be vulnerable to EM pickup. These sources are all discussed in [4] so they will not be treated in detail here. Fortunately it is possible to measure the sum of almost all of the contributions to the noise floor under circumstances very similar to those of the normal noise measurements. The only change needed is the elimination of the laser. This is done by disconnecting the RF reference from the input to the sync controller and connecting it instead to the input of the filter after the monitor photodiode (see fig 3). Now the two inputs to the phase noise measurement system are derived from the same RF source, and any noise measured must arise in the measurement system itself. The only system component which is not included is the photodiode, which will be treated separately below.

One practical consideration in noise floor measurement is that when both inputs are fed from the same source it is not possible to use the beat note technique to derive the phase slope. The solution adopted here was to set the signal levels to match, as closely as possible, those used for the laser noise measurements. The same phase

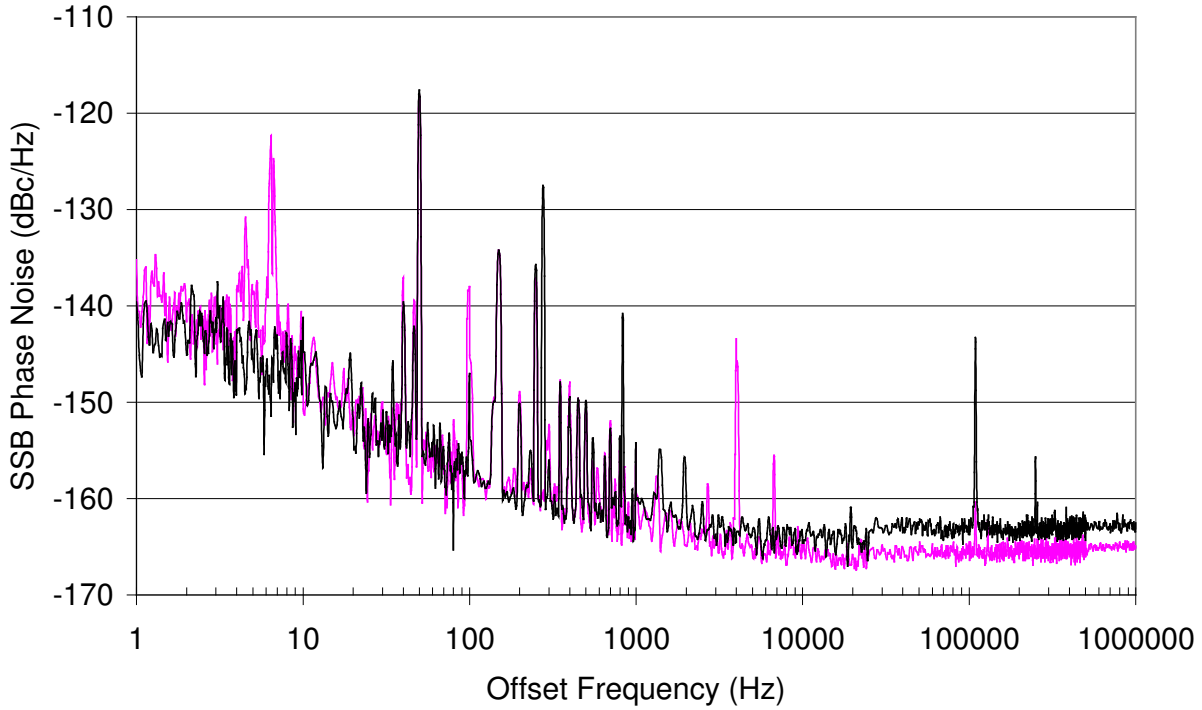


Figure 9: Two measurements of SSB phase noise floor for the HP3047A system and the external RF amplifiers and filter. Spur data are normalised to the spectrum analyser bandwidth.

slope value can then be used. This approach also has the advantage that any noise which is dependent on the signal level will be the same in both tests. The actual signal levels, measured at the input sockets to the HP3047A, were 15dBm (1.26V rms) at the reference input and 9.8dBm (0.69V rms) at the signal input.

The results of the noise floor measurement are shown in fig 9. They are presented with the HP3047A's spur corrections removed i.e. in the same format as fig 8b). The two traces were taken on separate dates approximately two months apart. Both traces show the same basic features. The underlying broadband noise falls smoothly from about –140dBc/Hz at an offset frequency of 1Hz to about –164dBc/Hz for offset frequencies above 5kHz. A number of spurs are visible at harmonics of the 50Hz ac line frequency and also at other distinct frequencies. Some (e.g. the pink ones at 6.5Hz and 4.1kHz and the black ones at 275Hz and 250kHz) are only present in one trace. Equation (2) can be used to convert the phase noise spectra into equivalent timing jitters. The results across the full spectral range from 1Hz to 1MHz are 16fs rms and 22fs rms for the pink and black spectra respectively. In each case the bulk of the noise is in the final spectral decade, between 100kHz and 1MHz. The contributions from all frequencies below this are just 7fs rms and 8.05fs rms respectively.

While these results are much smaller than the laser jitter (see below) and therefore do not need to be improved for the current measurements, it is useful to consider what might be done if improvements were required. The first approach would be to increase the input signal levels. Some fraction (perhaps most) of the noise floor is independent of these, so increasing the signals will automatically increase the signal-to-noise ratio, S/N. Noise floor measurements made in dBc are in fact S/N measurements, so improving S/N will lower the noise floor. The M9H mixer in the HP3047A system is

designed to operate with 20dBm input on the LO port. An increase from the current 15dBm level would lower the noise floor by up to 5dB which would reduce the jitter floor (measured in femtoseconds) by almost a factor of two. The second technique for improving the jitter sensitivity is to use harmonics of the reference and laser pulse frequencies. The conversion from noise floor to timing jitter floor involves division by the operating frequency, ω_0, and if this can be raised then the jitter floor can be reduced. The use of harmonics has already been mentioned in Section 3 where it was presented in contrast to the quadrature approach. But in fact it should be possible to combine the two techniques. Provided relatively low harmonics are used, so higher-order terms do not distort the results, a reduction in the jitter floor proportional to the harmonic number should be possible (but see the shot noise discussion below).

When laser noise is being measured the noise floor will be raised by an additional contribution from photodiode shot noise. Starting from the Schottky formula [5] for the noise current, I_{sh}, associated with a DC current I, in bandwidth B:

$$I_{sh} = (2qIB)^{½} \qquad (3)$$

it can easily be shown that the ratio of the total shot noise power to the carrier power is inversely proportional to the current, with a value of –155dBc at 1mA. It is explained in [4] that the shot noise contribution to the SSB phase noise is 6dB below this.

The 9.8dBm signal level measured at the input to the HP3047A corresponds to a filtered photodiode signal of –5.2dBm (the RF amplifier shown in fig 6 has 15dB of gain). The relatively slow response of the photodiode, which was irradiated with laser pulses which were essentially δ-functions in the time domain, meant that only the first 3-4 harmonics of the laser pulse frequency were present in its output. A simple Fourier analysis of the pulse amplitude shows that the ratio of the power in the DC component to that in the 81.25MHz term is approximately 0.8 so, given the power at 81.25MHz, the DC power can be estimated to be -6.2dBm. In a 50Ω circuit the DC current from the photodiode is therefore ~2.2mA. The total shot noise associated with this current is –158.5dBc and the SSB phase noise element is –164.5dBc.

A comparison with fig 9 shows that adding in the shot noise does not raise the overall noise floor significantly for the measurements reported here. However if the other noise terms were to be reduced, as described above, it would quickly become necessary to reduce the shot noise too. This can only be done by raising the signal level from the photodiode i.e. by exposing it to higher laser intensity. The data in fig 7 show that the diode output can be increased by at least a factor of 3 from the present level (0.69V rms from the RF amplifier) without compromising linearity. This would give nearly 5dB reduction in the shot noise. It would also increase the carrier level at the HP3047A, with a consequent reduction in the instrumental noise floor. Initial impressions during the linearity tests were that even at the 2V rms level the signal from the photodiode/filter/amplifier was stable for at least a minute or so. This suggests that heating effects were not serious. However this would need to be confirmed before high power operation was undertaken.

Shot noise considerations may limit the use of higher harmonics, proposed above. If the instrumental noise floor, measured in dBc, is to be kept low then the carrier level must be maintained. To do this as the harmonic number increases requires the use of faster (i.e. smaller) photodiodes to supply the input signal. Saturation and thermal

effects will lower the limit on average current as the photodiode size is reduced. As the average current falls the shot noise will increase. At some point the gains made by operating at higher frequency will be cancelled out by the increases in the overall noise floor.

In summary, the phase noise measurement system as currently set up has the capacity to measure timing jitter over the range 1Hz-1MHz with a few tens of femtoseconds' resolution. This is more than adequate for characterising the ERLP photoinjector laser in its present state. Straightforward improvements should reduce the noise floor and, perhaps, increase the sensitivity to the point where timing jitters below 10fs can be measured.

One remaining practical point is that the HP3047A system, while currently performing extremely well, is commercially obsolete. The individual spectrum analysers are still supported by Agilent and can be maintained both by them and by a number of third-party providers. But the front end hardware is no longer supported and any repair/calibration is only available on a best-efforts basis. The computer control system is completely unsupported and, indeed, has already had to be ported away from its original platform. As far as we are aware no direct replacement for this fully-integrated system exists, although enquiries with a number of suppliers are continuing.

4.2 Laser System

The phase noise spectrum of the laser measured with respect to the 81.25MHz reference RF is shown in fig 10. A comparison with fig 9 reveals that the laser noise is well above the noise floor of the HP3047A and its associated RF amplifiers and also exceeds the photodiode shot noise. So for the purposes of data analysis the contribution from the noise floor is insignificant. The timing jitter, calculated using equation (2) and integrating over the full range from 1Hz to 1MHz is 480fs rms. This is a factor of two below the system specification (1ps rms) and is more than adequate for ERLP operation.

The measured noise spectrum has a number of distinct features. One is the collection of spurs between ~30Hz and ~1kHz. The details of these, along with an isolated additional one at 45.5kHz, are given in Table 1. They are shown in fig 10 not at their absolute power levels, but normalised to the analyser bandwidth. Most of them are harmonics of the 50Hz mains frequency but the ones at 29Hz, 630Hz and 45.5kHz must have other sources. The first two may be due to acoustic/vibrational disturbances of the laser. The 45.5kHz one may be pickup from a high-frequency switch-mode power supply. The mains-related spurs could also arise from psu noise. Unlike all the other noise contributions these spurs are almost certainly coherent with one another. Without knowing their relative phases it is not possible to determine the overall 50Hz waveform, but there is some evidence from the sync controller's Phase output that it has the form shown in fig 11 i.e. short spikes of alternate polarity separated by relatively flat regions. Fig 11 was generated by taking the measured spur powers and combining them with a $\pi/2$ phase shift between the even and odd harmonics. The waveform is characteristic of pickup from a power transformer's EM field, with the spikes resulting from the short bursts of current which flow in transformer/rectifier/capacitor circuits. The most likely way in which this noise could

influence the laser output is, in fact, through the synchronisation system itself.

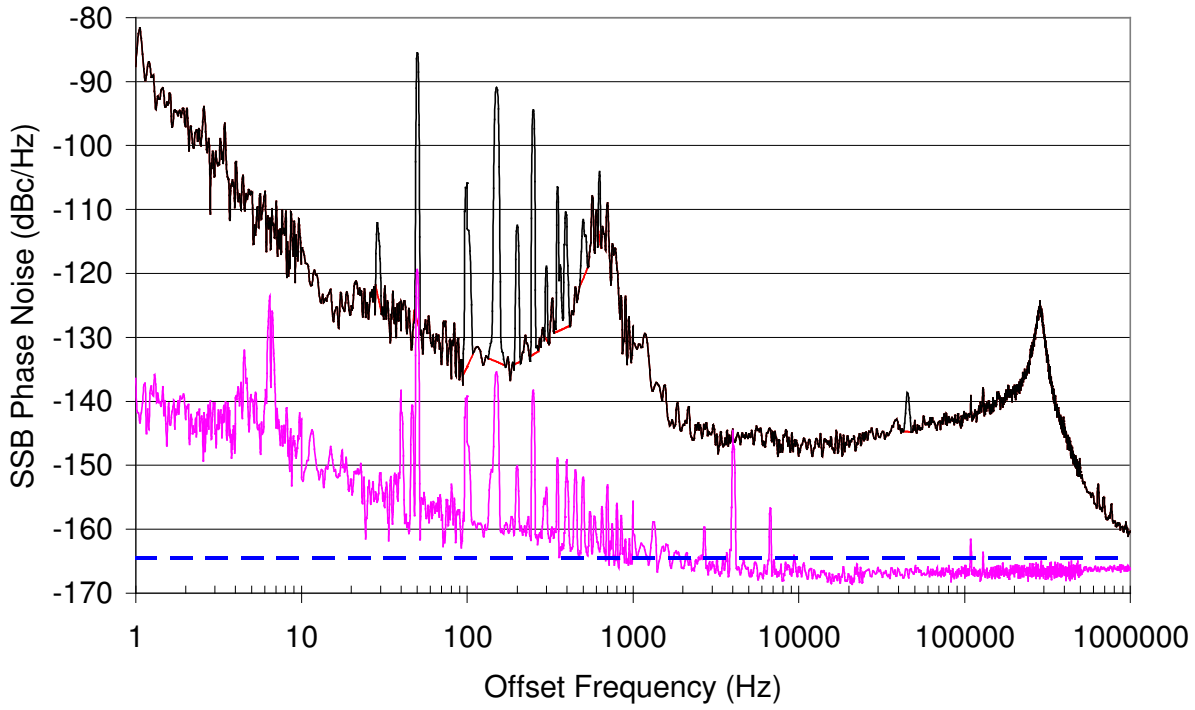


Figure 10: SSB phase noise of the ERLP photoinjector laser with spur data normalised to the spectrum analyser bandwidth (black) and with spur data removed (red interpolations). The pink trace shows the measured instrumental noise floor and the dashed blue line the calculated photodiode shot noise.

Spur No	Frequency (Hz)	Relative Power (dBc)
1	29	-112
2	50	-84
3	100	-104
4	150	-82
5	200	-104
6	250	-86
7	300	-110
8	350	-98
9	400	-102
10	500	-100
11	630	-92
12	45,500	-111

Table 1: Spurs present in the ERLP photoinjector laser SSB phase noise spectrum. The third column shows total power, not normalised to analyser bandwidth.

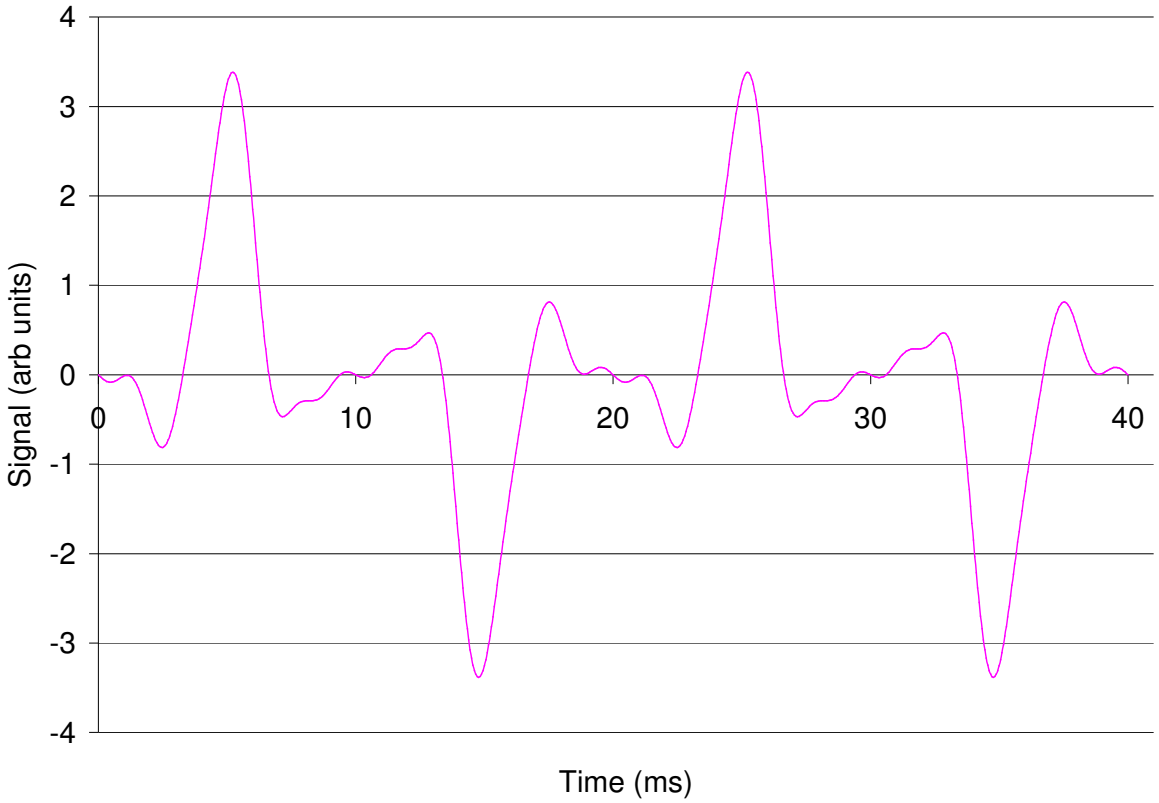


Figure 11: Waveform synthesised from the mains-related spurs measured in the ERLP phase noise spectrum.

The main electrical circuits for the laser are relatively high-current and low-impedance and therefore resistant to noise pickup. But this is not the case for the front end electronics in the synchronisation circuit where the small signals corresponding to the laser's phase error are produced. These signals are amplified and fed back to correct the laser timing. However if the electronics should pick up noise then this will be interpreted as a laser timing error and the circuit will attempt to correct it. The result is that the noise will actually be *imposed* on the laser timing and will appear on the phase noise measurements.

Attempts were made to identify the physical source of the 50Hz noise by disconnecting individual units from the mains and powering them from a battery-powered uninterruptible power supply (UPS). The UPS generated a 230V ac output whose frequency was close to 50Hz, but slightly different from the mains value. If an oscilloscope triggered from the AC line was used to observe the Phase waveform then the 50Hz component would stay static until its source was connected to the UPS, at which point it would begin to move slowly across the screen. This technique confirmed that the noise source was inside the sync controller itself.

The 50Hz noise makes a significant contribution to the overall timing jitter. It can be shown that the rms value of the jitter is independent of whether the spurs are coherent or not. So it can simply be measured by comparing the noise spectra with and without spurs (similar to the black and red traces in fig 10, except that only the mains-related spurs should be separated out). The result is that there is 320fs rms timing jitter associated with the mains spurs. Assuming the waveform of fig 11, this corresponds

to a peak-to-peak timing variation of 1.7ps. If this could be eliminated the remaining timing jitter would fall from 480fs rms to 360fs rms. Elimination would involve reducing the pickup in whichever electronic circuit is experiencing the problem. In a commercial system this might not be easy to do. Alternatively, given that the ERLP is pulsed at rates which are sub-multiples of 100Hz and that the macropulse lengths are relatively short (<100μs), it should in principle be possible to lock the time-structuring system to the mains frequency. Macropulses would then always occur at the same points in the noise cycle e.g. at the zero-crossings in fig 11. This should eliminate the effects of the noise without having to eliminate the noise itself.

The broadband underlying noise falls from -83dBc/Hz at 1Hz offset to -160dBc/Hz at 1MHz. At the lower frequencies the laser's intrinsic noise will have been strongly suppressed by the PLL synchronisation system. The broadband noise does not fall monotonically but has two broad peaks, one at ~700Hz and one at ~300kHz.

The peak at 700Hz, which actually runs from ~250Hz to ~1.5kHz, may have more than one source. When an audio system consisting of a sinewave generator, an amplifier and a loudspeaker was switched on in the room a spur corresponding to the audio frequency appeared on the laser noise spectrum. Clearly the sound was exciting some response in the laser structure which, in turn, was inducing phase noise on the output pulse train. As the audio frequency was scanned from <100Hz to >1kHz the size of the corresponding spur varied by as much as a factor of 5. There seemed to be broad resonances at certain frequencies, including several strong ones between 500Hz and 800Hz. When stimulated by the low-level acoustic noise present in the room at all times these features may be responsible for part of the 700Hz peak. However it is difficult to be quantitative about this as the audio system was crude and acoustic levels may also have been influenced by room and loudspeaker resonances. The coupling to the laser may also have depended on the position of the loudspeaker and the direction in which it was pointing. In an attempt to reduce acoustic effects the top plate of the laser head was covered in self-adhesive vibration damping material. No significant effect was seen on the amplitude or shape of the 700Hz peak which suggests that if acoustic noise was making a contribution to it then the coupling path was not via the laser top plate.

The influence of acoustics and vibration can be significant, however. The data in fig 10 were taken with only the normal, low-level background noise in the laser room. Attempts to reduce this further, for example by switching off equipment fans where possible and by ensuring that the doors of all equipment racks were closed, made no detectable difference to the measured phase noise. But if noise levels were raised, even by talking near the laser head, very definite effects were seen. Because they were transient they were easier to observe with the Phase monitor than with the HP3047A system. Snapshot measurements of the Phase signal showed that talking could increase the rms timing jitter by hundreds of femtoseconds. A similar effect occurred when the flow rate of the cooling water through the laser baseplate was increased. The normal flow rate is ~5-10ml/sec. Raising this, perhaps by a factor of 3-5, resulted in the rms timing jitter as measured on the Phase monitor increasing again by hundreds of femtoseconds. Presumably this was caused by turbulence in the coolant flow channels generating vibration in the laser body. Detailed analysis was not carried out but the noise appeared to be occurring predominantly in the 100Hz-2kHz range. A third example of vibration-induced phase noise occurred when the laser

safety shutter, which is mounted on the aluminium gantry, inadvertently came into contact with the laser head (they are normally separated by a gap of ~1mm). Vibrations from the time-structuring hardware, which can be felt by hand in the gantry, were coupled into the laser and immediately raised the timing jitter to levels above 1ps rms.

The low frequency side of the 700Hz phase noise peak corresponds to the range over which the gain of the synchronisation PLL rolls off. This is almost certainly not a coincidence. If the gain rolls off faster with frequency than the intrinsic noise falls, then the residual noise with the PLL feedback system operating will increase over this frequency range. In addition a more subtle process may be occurring. The general effect of the PLL is to reduce noise by a large factor over a large frequency range. Indeed this is the whole point of using it. But the tendency for PLLs to raise the noise *above* the intrinsic level over a small range around the roll off frequency has also been reported elsewhere [6]. This effect may also be contributing to the 700Hz peak.

The cause of the higher frequency noise peak, near 300kHz, has not been identified with certainty. It is beyond the range of any plausible mechanical vibrations. There are no local sources of external noise at this frequency and the broad linewidth does not suggest an artificially "tuned" source. The most plausible explanation is relaxation oscillation in the laser medium. The fluorescence lifetime of Nd:YVO_4 is ~100μs. The upper state lifetime under laser conditions will be rather less than this because of the laser action itself, but the high saturation intensity means that the lifetime reduction will not be very large. It might therefore be expected that any variations, for example in the laser pump power, would be damped out at frequencies above ~10kHz. But in the high intensity regime the laser population dynamics are controlled by two characteristic lifetimes. The laser upper state lifetime is one. The other is the photon lifetime in the laser cavity. This is of the order of the cavity Q multiplied by the round-trip time (12.3ns) and might typically be ~100ns. Interactions between the photon number density and the laser inversion density lead to oscillations of both populations at frequencies between the two inverse lifetimes. An introduction to relaxation oscillation is given in [7] and the effects on intensity noise are reported in [8]. An example of measured relaxation oscillation noise is reproduced from [8] as fig 12. The resemblance between this feature and the 300kHz peak in fig 10 is clear.

The 300kHz peak is another major contributor to the overall timing jitter. Its breadth and its shallow wings make quantitative assessment difficult, but it must account for the bulk of the jitter between 30kHz and 500kHz. Integrating the fig 10 data over this range results in a contribution of 320fs rms. A linear interpolation between the end points yields an underlying jitter of just 75fs rms. Replacing the 320fs figure with the 75fs one (in quadrature, of course) would reduce the overall jitter from 480fs rms to 365fs rms.

In practice reducing the effects of relaxation oscillation is difficult. The tendency to oscillate is an intrinsic property of the laser medium itself, with some media being more sensitive than others. The oscillation amplitude and frequency will depend on the chosen operating point (in particular the intracavity power) and on the size of the perturbations which drive the oscillation. The analysis in [8] shows that even with low-noise pumping from a single-element diode, relaxation oscillation cannot be eliminated – there will always be a driving term arising from vacuum fluctuations.

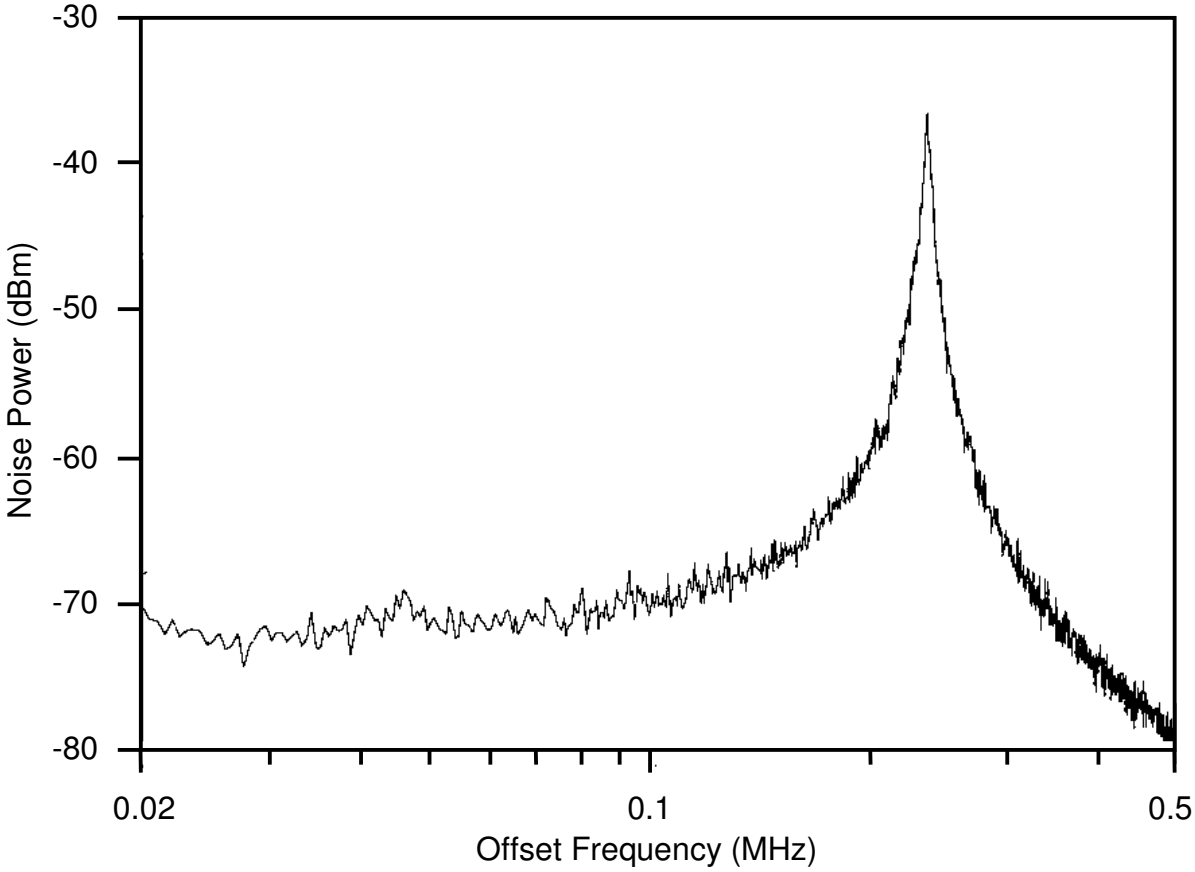


Figure 12: Intensity noise power measured in a CW diode-pumped Nd:YAG laser [8] showing a peak characteristic of relaxation oscillation.

When a diode laser array is used as a pump source, as is generally the case for high average power oscillators like the High Q system, the relaxation oscillation amplitude is significantly higher. Another feature of the High Q laser – the slow saturable absorber used to modelock it – is known to increase the relaxation oscillation amplitude by effectively reducing the damping [9].

The main effect of relaxation oscillation is to modulate the laser intensity. However the effect which most concerns us is the associated modulation of the laser's pulse timing i.e. the increase in the phase noise. The magnitude of this is affected by several factors, one of which is the choice of laser modelocking technique. As well as increasing the oscillation amplitude, the use of a slow saturable absorber can also increase the resulting phase noise through enhanced AM to PM conversion [10]. In these circumstances it is perhaps not surprising that what appears to be a relaxation oscillation noise peak should be so prominent in fig 10.

It has already been pointed out that the synchronisation performance of the laser system exceeds both the contract specification and also the level required for effective operation of the ERLP. However there are some practical operational features which do deserve to be mentioned. The first concerns the ability of the laser to phase lock to different RF sources. Only two types of source have been tested. The oven-controlled crystal oscillators (Wenzel Inc) have extremely low intrinsic noise. The laser locks very well to these, with the excellent results described above. It is also worth pointing out that the system typically stays locked for many hours, which is very important in an

accelerator application. However earlier in the programme attempts were made to lock to a noisier source – a Marconi Instruments model 2019A RF synthesiser - with worse results. Phase noise levels were higher when lock was achieved and there was a strong tendency for lock to be lost. Clearly the choice of a low-noise reference is important. It is also the case that the system will not lock reliably until it has reached a stable operating temperature, which takes approximately 45 minutes from switch-on. Over this period the internal components of the laser heat up and the cavity length increases, in fact by more than the range of either of the movable mirrors. Even when the required cavity length does come within range the phase locking is not immediately stable. The motor-driven mirror either does not move to compensate for any further thermal changes, so lock is lost, or if it does move it does so in a way which disturbs the lasing so badly that again lock is lost. The indications are that the motor does not attempt to move. Instead the feedback electronics start to drive the piezo mirror in a way which generates an audible whine. At the same time the Phase signal switches to a level corresponding to a loss of lock, but with a waveform whose shape is very non-sinusoidal. It is under these circumstances that the LED indictor on the sync controller front panel stays on, suggesting that the system is phase locked when in fact it is not.

5. CONCLUSIONS AND FUTURE WORK

During the course of this programme the ERLP photoinjector laser has been phase locked to the accelerator RF and is now routinely supporting accelerator development activities. With a low-noise reference source and under thermally stable conditions the locking can be sustained for periods of many hours. In addition a high-sensitivity broadband phase noise measurement system has been set up and characterised. It has been used to measure a laser timing jitter of 480fs rms with respect to the local RF over an offset frequency range of 1Hz-1MHz. Analysis of the noise spectrum has revealed that a mains-related feature and what appear to be laser relaxation oscillations are major contributors to the jitter. Vibrations and acoustics have been shown to influence the timing when their levels are increased above the normal background in the laser room.

Potential future activities include:

i. Location and reduction of the source of 50Hz noise in the synchronisation system. This will reduce the timing jitter significantly. The noise appears to come from one or other of the sync controller power supplies. A first step will be to extend the leads on these and establish, by moving them further away, whether the pickup comes directly from one of the transformers.

ii. Development of a machine protection system based on the sync controller Phase output. When the ERLP accelerating modules are brought into use the consequences of a loss of laser phase lock will become serious. Electrons will then enter the modules at essentially arbitrary times and, having acquired the “wrong” energy, will be lost through collisions with the walls or other machine components. They may, however, have sufficient energy to generate excessive ionising radiation dose or even to damage the machine in the process. It will therefore be necessary to shut the beam down as quickly as possible. Under normal circumstances the Phase output signal has an amplitude of just a few millivolts. This immediately

changes to a sinusoid with a peak-to-peak amplitude of ~20V when the sync controller loses lock. Detection of this and generation of a signal to switch the laser off (perhaps using the Pockels cell) should be straightforward.

iii. Extension of the HP3047A system's frequency range. The ultimate limit to the range of offset frequencies over which the HP3047A can work is set by the upper frequency limit of the spectrum analysers, which is 40MHz. When measuring pulse trains whose frequency is less than twice this the system carries out measurements up to half the pulse train frequency – the Nyquist limit, beyond which no further phase noise information is available. But when the pulse train frequency is higher than 80MHz, as it is for the High Q laser, a software feature limits the upper offset frequency to 1MHz which is the value used for the measurements in this report. In fact more information would be available if this feature could be switched off and the offset frequency extended to 40MHz. It is proposed to modify the software to allow this.

iv. Improvement of the HP3047A system's timing jitter sensitivity. Techniques for doing this, by increasing the RF reference amplitude, increasing the photodiode current (to reduce the shot noise) and using higher harmonics (to improve the timing jitter to phase noise ratio) have been described above. These should soon be implemented.

v. Confirmation of timing jitter measurements using optical techniques. Other lasers, in addition to the photoinjector laser, are now being brought on line in the ERLP laser room. These can also be phase locked to the 81.25MHz accelerator RF. Their synchronisation to one another can be measured with high sensitivity and low long-term drift using optical cross-correlation. The results can then be compared with individual measurements taken using the HP3047A system. The comparison should allow the calibrations of the two different approaches to be confirmed.

vi. Transfer of the synchronisation from the laser room to the electron gun. At present the sync controller is used to lock the laser pulse timing, as measured inside the laser head, to the reference RF, as measured at the output of the cable in the laser room. In fact the machine performance depends on the synchronisation between the electron bunches as they enter the RF-powered elements and the RF field inside those elements. Accurate measurement of the electron bunch timing is not straightforward, but it should at least be possible to measure the laser pulses much closer to the photocathode than at present. As mentioned above measurement of the intracavity RF fields can also be complicated. But the LLRF can be measured as it leaves the master oscillator. Moving these measurement points would allow the synchronisation system to compensate for jitter and drift in the laser beam transport optics and would eliminate the need to transfer the reference RF over the long cable to the laser room. Instead the much slower signals used to control the mirror positions could be taken to the laser.

    Many elements of this scheme are already in place and several have been tested. The main laser beam is sampled for diagnostic purposes just below the electron gun and this might seem to be an obvious place for a timing reference pick-off. Unfortunately this is not practical because the main beam has been time-structured by this point and cannot therefore be used to generate the required CW error signal. It is therefore planned to pick off a CW timing beam before the

time-structuring system and transport this along the same optical path as the main beam. The optical elements needed to do this and the beam itself are both shown in fig 3. The timing beam is coloured red since it has not been frequency doubled to the green. This allows it to be separated from the main beam by a dichroic mirror just before the gun. It also prevents any CW beam which leaks through to the photocathode from releasing any electrons (Cs:GaAs cathodes are insensitive to 1.06μm light). A successful synchronisation test using the timing beam in the laser room has been carried out.

The cable for the movable mirrors must carry both high voltage signals for the piezo element and relatively high current ones for the drive motor. A 50m cable with the required capacity has been constructed and successfully tested. For this experiment the sync controller was moved close to the gun and the reference RF supplied over a cable just 2m long. The only missing element was the local photodiode sampling the timing beam (a diode in the laser room was used). There were two reasons why local laser timing was not practical. Firstly the dichroic beam splitter needed to separate the timing and main beams was not available. Secondly the scheme depends for its success on having a very stable mount for the photodiode, since changes in the position of this will directly affect the timing. A suitably stable platform was also not available at the time the test was carried out. Once the beam splitter and platform have been put in place the transfer of the synchronisation point from the laser room to the gun region should quickly follow.

REFERENCES

1 M W Poole and E A Seddon, *4GLS and the energy recovery linac prototype project at Daresbury Laboratory*, Proceedings of PAC 2005 p431 (2005)

2 J F Orrett et al, *IOT Testing at the ERLP*, Proceedings of EPAC 2006 p1382 (2006)

3 G Priebe et al, *Inverse Compton backscattering source driven by the multi 10 TW laser installed at Daresbury*, paper 6702-14, SPIE Optics + Photonics 2007 (2007)

4 R P Scott, C Langrock and B H Kolner, *High-dynamic-range laser amplitude and phase noise measurement techniques*, IEEE J Sel Topics in QE **7** (4) 641 (2001)

5 See e.g. H W Ott, "Noise Reduction Techniques in Electronic Systems", publ Wiley, 2nd edn, p238 (1987)

6 See e.g. the third entry under "Complications" on this web page http://www.wenzel.com/documents/measuringphasenoise.htm

7 A E Siegman, "Lasers", publ OUP, chapter 25, (1986)

8 C C Harb et al, *Intensity-noise dependence of Nd:YAG lasers on their diode-laser pump source*, JOSA B **14** (11) 2936 (1997), data abstracted from fig 12

9 A Schlatter et al, *Q-switching stability limits of continuous-wave passive mode locking*, JOSA B **21** (8) 1469 (2004)

10 R Paschotta, *Noise of mode-locked lasers Part II: timing jitter and other fluctuations*, Appl Phys B **79** (2) 163 (2004)